Med Biol Eng Comput (2014) 52:29–43
DOI 10.1007/s11517-013-1114-x

ORIGINAL ARTICLE

Denoising performance of modified dual-tree complex wavelet transform for processing quadrature embolic Doppler signals

Gorkem Serbes · Nizamettin Aydin

Received: 2 January 2013 / Accepted: 1 September 2013 / Published online: 19 September 2013

Abstract Quadrature signals are dual-channel signals obtained from the systems employing quadrature demodulation. Embolic Doppler ultrasound signals obtained from stroke-prone patients by using Doppler ultrasound systems are quadrature signals caused by emboli, which are particles bigger than red blood cells within circulatory system. Detection of emboli is an important step in diagnosing stroke. Most widely used parameter in detection of emboli is embolic signal-to-background signal ratio. Therefore, in order to increase this ratio, denoising techniques are employed in detection systems. Discrete wavelet transform has been used for denoising of embolic signals, but it lacks shift invariance property. Instead, dual-tree complex wavelet transform having near-shift invariance property can be used. However, it is computationally expensive as two wavelet trees are required. Recently proposed modified dual-tree complex wavelet transform, which reduces the computational complexity, can also be used. In this study, the denoising performance of this method is extensively evaluated and compared with the others by using simulated and real quadrature signals. The quantitative results demonstrated that the modified dual-tree-complex-wavelet-transform-based denoising outperforms the conventional discrete wavelet transform with the same level of computational complexity and exhibits almost equal performance to the dual-tree complex wavelet transform with almost half computational cost.

Keywords Quadrature signal · Complex wavelet transform · Denoising · Embolic signals

G. Serbes
Biomedical Engineering Department, Bahcesehir University, Çırağan Caddesi, Osmanpaşa Mektebi Sokak No: 4–6, 34353 Beşiktaş, Istanbul, Turkey
e-mail: gorkem.serbes@bahcesehir.edu.tr

N. Aydin (✉)
Computer Engineering Department, Faculty of Electrical and Electronics, Yildiz Technical University, Davutpasa, 34220 Esenler, Istanbul, Turkey
e-mail: naydin@yildiz.edu.tr

1 Introduction

Asymptomatic circulating cerebral emboli, which are particles larger than red blood cells, can be detected by transcranial Doppler ultrasound [33]. In certain conditions, such as carotid artery stenosis, asymptomatic embolic signals appear to be markers of increased stroke risk and may be useful in patient management [22]. These embolic signals can be extracted from quadrature Doppler signals, which are obtained at the end of quadrature demodulation process [15]. In demodulation stage, the returning Doppler signal is multiplied by two reference signals that have 90° of phase shift between them. Later, the high-frequency components are removed by low-pass filtering, and these processes result in two components, the in-phase and the quadrature-phase components, which are within the audio frequency range and have 90° phase difference. The information concerning flow direction, which is encoded in the phase relationship between in-phase and quadrature-phase channels, can be extracted by further decoding these signals [4].

Traditionally, for detecting embolic signals, individual recordings are analyzed visually, which is a time-consuming process. The average duration of recording emboli is likely to be at least 30 min. Therefore, for a clinically useful detection technique, an automated detection system is needed [21]. Although there are attempts to design and

implement automated systems for emboli detection [6, 16, 24, 26], a major problem with clinical implementation is the lack of reliability. A Doppler ultrasound signal detected by the transcranial Doppler ultrasound system used for emboli detection is composed of embolic signal, Doppler speckle (signals caused by red blood cell aggregates) and artifact (signals caused by tissue movement, probe tapping, speaking and any other environmental effects). A reliable automated emboli detection system should ideally eliminate Doppler speckle and artifact while enhancing embolic signals. In practice, the most significant improvement in an online system may be achieved by efficiently reducing unwanted signal components by using denoising techniques, such as speckle removing in Doppler imaging [1], a matching pursuit algorithm-based denoising method in [36] and an adaptive pulse-coupled-neural network-based speckle reduction method in [20].

Denoising, which involves in estimating the unknown signal of interest from the available corrupted data, is the first preprocessing step in analyzing biomedical signals obtained from physiological processes [11]. The discrete wavelet transform (DWT) is widely used for reducing noise levels in noisy signals. The DWT denoising process involves in transforming the signal into scale domain, zero filling or modifying selected wavelet coefficients by some criteria, which also named as wavelet threshold, and then transforming the manipulated signal back into the time domain [12]. In literature, two main nonlinear thresholding approaches, namely hard thresholding and soft thresholding, have been widely used. In the hard thresholding, the wavelet coefficients lower than a threshold value are set to zero, while in soft thresholding, not only the small coefficients are set to zero but also the larger ones are shrinked by an amount equal to the threshold. Soft thresholding is based on the idea that each coefficient of the transform consists of partly the original signal and partly the noise. As a consequence, the transition between small coefficients and large coefficients is continuous in soft thresholding. This results in fewer corruptions in the analyzed signal. Therefore, in our study we used soft thresholding as the shrinkage function.

The choice of threshold values plays a vital role in the denoising performance of wavelet processes. Several approaches such as universal threshold (also named as VisuShrink) [12], SureShrink [13] and Minimax [14] for choosing the optimum threshold value for analyzed signal have been proposed in literature. In this study, because of its simplicity in calculation and low computational cost, VisuShrink method for threshold selection approach was used. This method uses a single universal threshold for all scales, which is calculated from the first-band detail coefficients due to most of noise components appearing in that band. VisuShrink method yields estimates that are near-optimal in minimax sense, and the resulting estimate is very smooth with a pleasant visual appearance [35]. For a more detailed explanation of wavelet-based denoising methods, review papers in [9, 19, 34] can be examined.

There is also a complex DWT named as dual-tree complex discrete wavelet transform (DTCWT) having near-shift invariance properties with a reasonable computational complexity [17, 29]. In [30, 32], a modified version of DTCWT (MDTCWT) was proposed for processing quadrature Doppler signals. This transform represents signal into different scales and also inherently provides forward and reverse flow components from quadrature signals at the end of the synthesis process. Similar to the conventional DWT, the MDTCWT algorithm can also be utilized to implement denoising. In denoising quadrature signals, instead of two DWTs or two DTCWTs, a single MDTCWT can be utilized providing both directional information extraction and denoising with almost the same computational complexity of the DWT and half of the DTCWT. The details of MDTCWT can be found in [32]. A preliminary study on the denoising performance of MDTCWT was presented in [31]. In this study, the denoising performance of MDTCWT is extensively evaluated and compared with the DWT and the DTCWT by using simulated and real quadrature signals.

The remaining of the paper is organized as follows: Sect. 2 gives information about quadrature signals and embolic signals. Section 3 reminds the basics of MDTCWT. Section 4 describes the materials and methods. Section 5 presents the results, and finally, Sect. 6 provides the discussions and conclusions.

2 Quadrature signals and embolic signals

2.1 Quadrature signals

Quadrature signals, which are dual-channel signals, are obtained at the detection stage of the systems employing quadrature demodulation technique. In-phase and quadrature-phase components of quadrature signals can mathematically be assumed as real and imaginary signals [4]. Then, a quadrature signal can be modeled as $y(n) = D(n) + jQ(n)$, where $D(n)$ is in-phase and $Q(n)$ is quadrature-phase components of the signal. Considering Doppler ultrasound systems used in blood flow detection, the information concerning flow direction is encoded in the phase relationship between $D(n)$ and $Q(n)$. They have 90° phase difference. Although there are a number of methods for extracting directional signals from the quadrature signals, the phase filtering technique (PFT) based on HT is the most widely used method [4]. Therefore, in this work, the simulated reconstructed denoised directional outputs of

MDTCWT, DTCWT and DWT were compared with the noise-free outputs of the PFT for the calculation of respective root mean square error (RMSE) and signal-to-noise ratio (SNR) values.

2.2 Embolic signals

Stroke is a condition causing partial or total paralysis, or death. The most common type of stroke occurs when a blood vessel in or around the brain becomes plugged. The plug can originate in an artery of the brain or somewhere else in the body, often the heart, where it breaks off and travels up the arterial tree to the brain, until it lodges in a blood vessel [22]. These travelling clots, which are particles larger than red blood cells, are called emboli.

The ability to detect asymptomatic circulating cerebral emboli with an automated system might allow the selection of patients who are prone to stroke and would particularly benefit from preventative treatment. Transcranial-Doppler-ultrasound-based systems can be used to detect asymptomatic circulating cerebral emboli. Additionally, in patients with stroke and more than one embolic source, such as unilateral carotid stenosis and atrial fibrillation, Doppler ultrasound recording from different sites would allow determination of which source is actively embolizing [25].

Embolic Doppler ultrasound signals are special blood flow signals with the following properties. They have some distinctive characteristics when compared to high-intensity signals from normal blood flow and artifacts caused by tissue movement, probe tapping, etc. They appear as increasing and then decreasing in intensity for a short duration [2]. Embolic signals are unidirectional and usually contained within the flow spectrum. The spectral content of an embolic signal is also time dependent.

3 Modified dual-tree complex wavelet transform

The DTCWT was developed to overcome the lack of shift invariance property of ordinary DWT. Conventionally, prior to applying the DTCWT to the quadrature signals, first the forward and the reverse signal components must be extracted from the quadrature signals, and then two DTCWTs should be applied. However, a modified version of the DTCWT algorithm (MDTCWT) that results in a reduced computational complexity was proposed in [32]. This is attained by combining the part of the PFT with a modified DTCWT. The details of the DTCWT implementation can be found in [17, 29]. In DTCWT, a real signal is applied to both trees for decomposition, and the outputs of both reconstructed trees are added at the end of reconstruction stage. The analysis part of the DTCWT for three levels is illustrated in Fig. 1.

In the MDTCWT, two modifications are made to the conventional DTCWT as illustrated in Figs. 2 and 3. At the analysis stage, instead of applying the quadrature signal to both trees, the in-phase part is applied to the real tree through a HT filter introducing a 90° phase shift into the real part of the signal, and the quadrature-phase part is applied to the imaginary tree directly. At the reconstruction stage, in addition to adding the outputs of reconstructed real and imaginary trees giving the signals caused by the flow in one direction, they are also subtracted resulting in the signals caused by the flow in the other direction. More detailed discussion and analytic expression on MDTCWT can be found in [30, 32].

At the analysis and synthesis stages of MDTCWT, the same filter-bank pairs as in the DTCWT are used. Therefore, the MDTCWT inherits near-shift invariance property of the DTCWT. Because embolic signals are short duration and unidirectional quadrature signals, the phase information

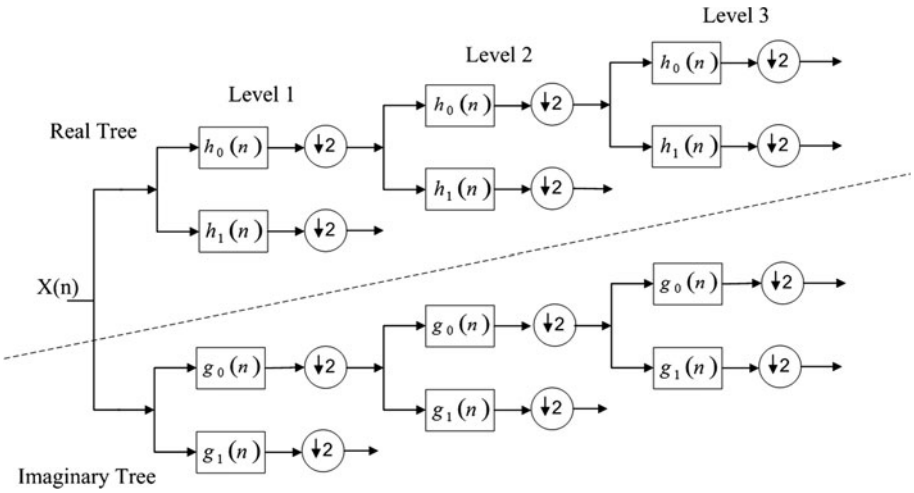

Fig. 1 Analysis stage of DTCWT algorithm

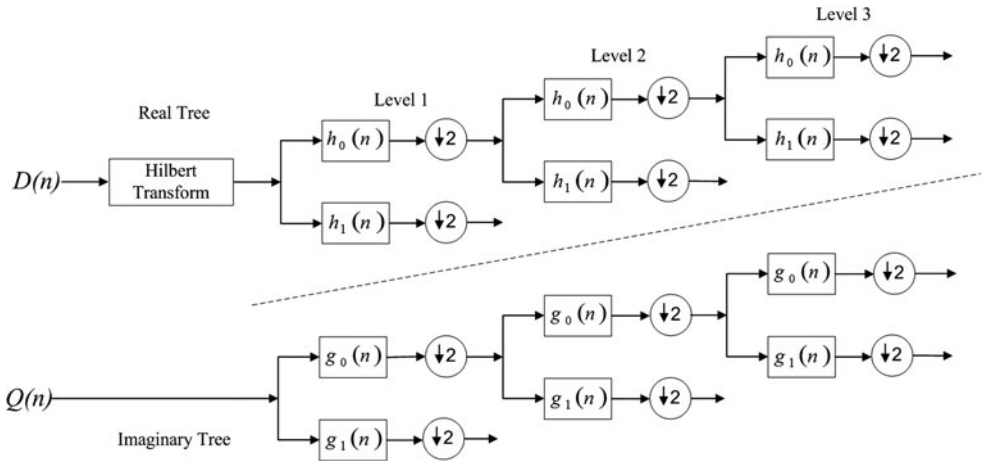

Fig. 2 Analysis stage of MDTCWT algorithm

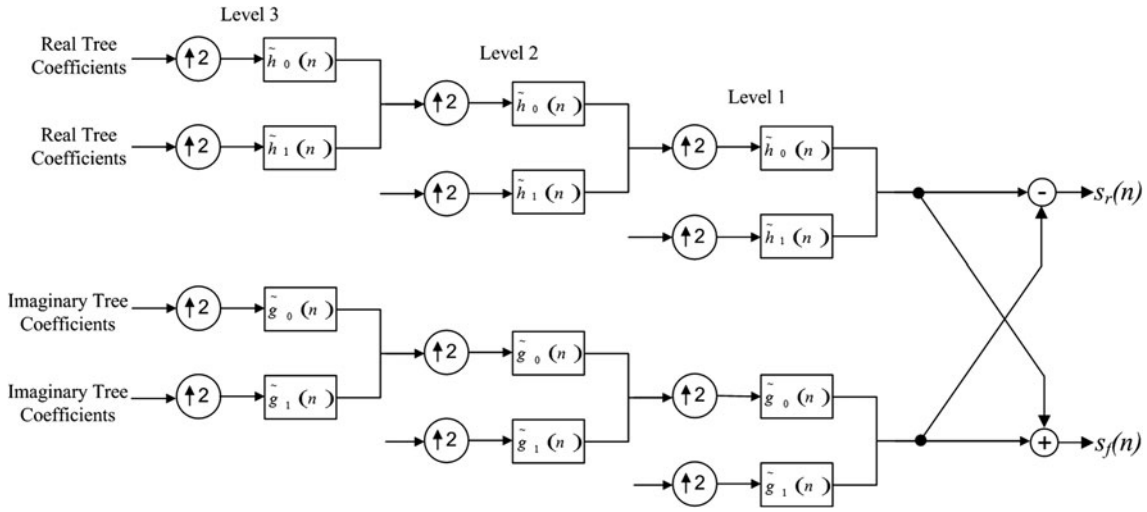

Fig. 3 Synthesis stage of MDTCWT algorithm ($s_f(n)$ represents the signals caused by the blood flow in forward direction, and $s_r(n)$ represents the signals caused by the blood flow in reverse direction)

should not be distorted during the analyses as the flow direction is encoded in the relationship between in-phase and quadrature-phase components. Therefore, the near-shift invariance property of MDTCWT is very important while processing embolic signals.

4 Materials and methods

In order to evaluate the denoising performances of all the three methods quantitatively, a noise-free simulation signal in quadrature format was constructed by using sinusoidal signals. Later, a random synthetic Gaussian noise is added to noise-free quadrature signal, resulting in the noisy signal. Then the noisy simulation signals were denoised by using MDTCWT, DTCWT and DWT. The outputs of the three methods were subtracted from the noise-free outputs of the PFT [4] algorithm, and the differences were computed as RMSE and SNR values. RMSE is given as:

$$\mathrm{RMSE} = \sqrt{\frac{1}{N}\sum_{i=1}^{N}\left(X_i - \hat{X}_i\right)^2} \tag{1}$$

where $\hat{X}_i$ is the resulting denoised directional signal of the related method and X_i is the original directional signal without noise. SNR is defined as:

$$\mathrm{SNR} = 10\log_{10}\left(\frac{P_{\mathrm{signal}}}{P_{\mathrm{noise}}}\right) \tag{2}$$

where P_{signal} is the power of denoised signal and P_{noise} is the power of noise.

For an unbiased evaluation, comparison of the methods was made first by using a number of simulated signals with different frequency values, second by employing different threshold levels for denoising algorithm and lastly by setting the SNR of the simulated signal to three different levels (6, 8 and 10 dB). Finally, the average RMSE and SNR values were computed and compared.

Again, in order to evaluate the denoising performances of all three methods quantitatively and qualitatively, 25 quadrature embolic Doppler signals recorded from the patients were denoised by using MDTCWT, DTCWT and DWT. As a comparison parameter, embolic signal-to-background signal ratio (EBR) values for the three methods were calculated and compared. The EBR is a ratio between embolic signal's power and background noise level and is calculated as:

$$\mathrm{EBR} = 10\log\frac{A_{\mathrm{peak}}}{B_{\mathrm{avg}}} \tag{3}$$

where A_{peak} is the power at frequency with maximum power intensity. B_{avg} is the average power of the background intensity and calculated by time and frequency averaging of the time–frequency (TF) results.

Time–frequency representations of these signals were also obtained and plotted. In these plots instantaneous power (IP) [7] of noisy and denoised embolic signals was used in order to show the performance of three methods. Examples of IP of noisy embolic Doppler signal (thin) calculated from time domain quadrature signal, and embolic Doppler signals denoised by three algorithms (thick) are illustrated in Fig 4. In this figure %20 and %50 points of the signals give us the information about embolic signal onset (ESO) and half-width maximum (HWM) of the embolic signal, respectively. These concepts are explained in Sect. 4.2 in more detail.

For denoising process, as mentioned before in "Introduction" part, soft thresholding technique was used for both simulated signals and real embolic signals. In soft thresholding, after completing decomposition part of wavelet transform, all frequency subband coefficients that are less than a predefined threshold were set to zero and then the threshold was subtracted from the nonzero coefficients. Finally, the denoised coefficients were used in an inverse wavelet transformation to reconstruct the data set [28]. The soft thresholding can be defined as:

$$\hat{d}_j(k) = \begin{cases} \mathrm{sgn}\big(d_j(k)\big)\left(\left|d_j(k)\right| - T\right) & \left|d_j(k)\right| \geq T, \\ 0 & \left|d_j(k)\right| < T \end{cases} \tag{4}$$

where $\hat{d}_j(k)$ is the thresholded coefficients in jth level, T is the threshold, and sgn() represents the signum function.

In simulated signals, fixed threshold values were used for denoising. However, for real embolic signals, an optimum threshold value for each signal was calculated by using universal thresholding method. The details of universal thresholding method are mentioned in Sect. 4.2. In this respect, in this study the denoising performance of the

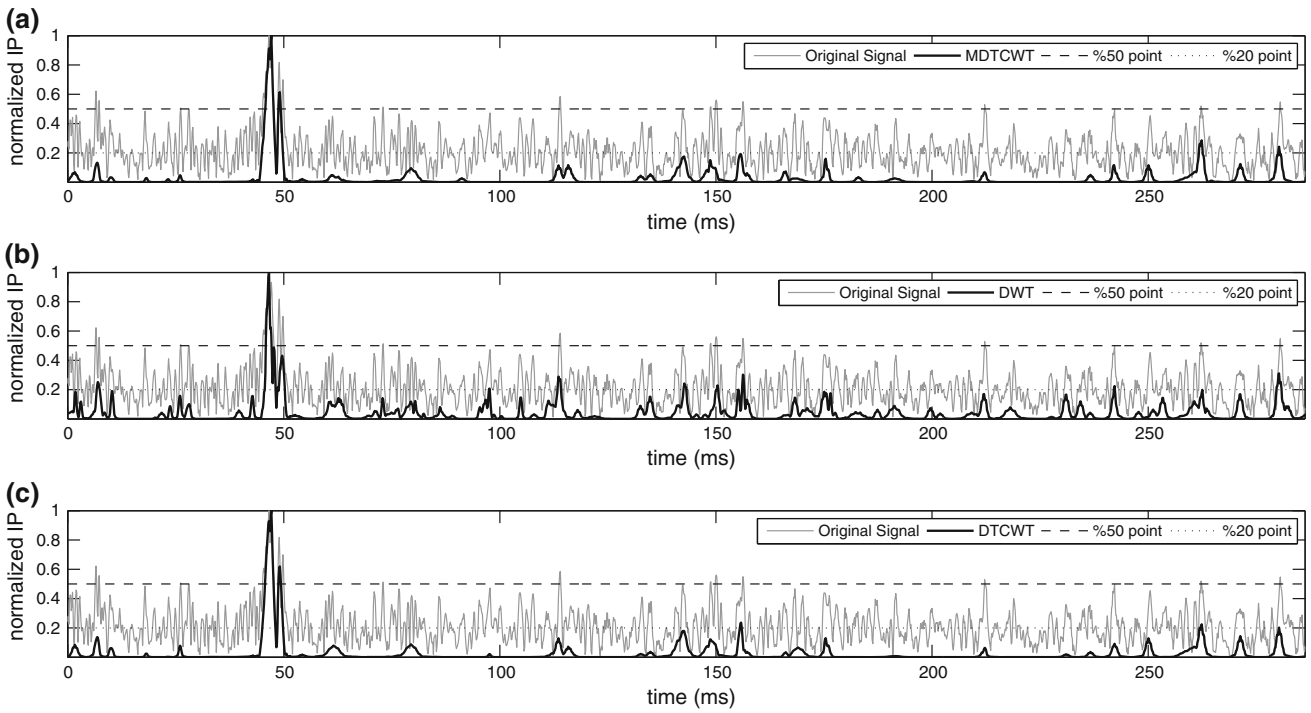

Fig. 4 Instantaneous power of **a** noisy signal and denoised signal with MDTCWT, **b** noisy signal and signal denoised with DWT, **c** noisy signal and signal denoised with DTCWT (*light line* noisy signal, *bold line* denoised signal)

MDTCWT was compared with the DWT and the DTCWT by using soft thresholding.

4.1 Simulated signals

The simulated quadrature signal contaminated with white Gaussian noise was constructed in Matlab program, and denoising process was implemented for the MDTCWT, the DWT and the DTCWT. Signal and noise model for quadrature signal can be given as:

$$y_n(n) = D_n(n) + jQ_n(n) \quad n = 1, \ldots, N \tag{5}$$

$$D_n(n) = (n) + g(n) \tag{6}$$

$$Q_n(n) = Q(n) + g(n) \tag{7}$$

where y_n is N point noisy quadrature Doppler signal and $g(n)$ is white Gaussian noise.

Time domain and frequency domain representations of a noise-free quadrature signal $y(n)$ constructed by using sinusoidal signals are illustrated in Figs. 5 and 6, respectively. Simulated quadrature signal containing the forward and reverse signal components was created by using the following equations, where A and B are the signal amplitudes, f_A and f_B are the frequency of the directional signals representing forward and reverse signals, and f_S is the sampling frequency.

$$D_n(n) = A\cos(2^*pi^*n^*f_A/f_S) + B\sin(2^*pi^*n^*f_B/f_S) + g(n) \tag{8}$$

$$Q_n(n) = A\sin(2^*pi^*n^*f_A/f_S) + B\cos(2^*pi^*n^*f_B/f_S) + g(n) \tag{9}$$

For the signal shown in Fig. 5, A is chosen to be twice as much as B. f_A and f_B are chosen to be 1 and 2 kHz, respectively.

In literature, it is well known that the frequency spectrum of a quadrature signal is one-sided [8]. Equations (8) and (9) represent an example of quadrature-phase and in-phase components of a quadrature signal. Considering properties of the Fourier transform [8], Fourier transform of a real-even signal will result in a real-even spectrum, a real-odd signal will result in an imaginary-odd spectrum, an imaginary-even signal will result in an imaginary-even spectrum, and an imaginary-odd signal will result in a real-odd spectrum. Depending on the phase difference between $D(n)$ and $Q(n)$, either positive or negative frequency parts of f_A and f_B cancel out during the Fourier transform operation. In this respect, Fourier transform of $y(n)$ will result in a one-sided spectrum (spectrum of f_A will appear only at positive frequency part, spectrum of f_B will appear only at negative part) as described in [3]. Therefore, in

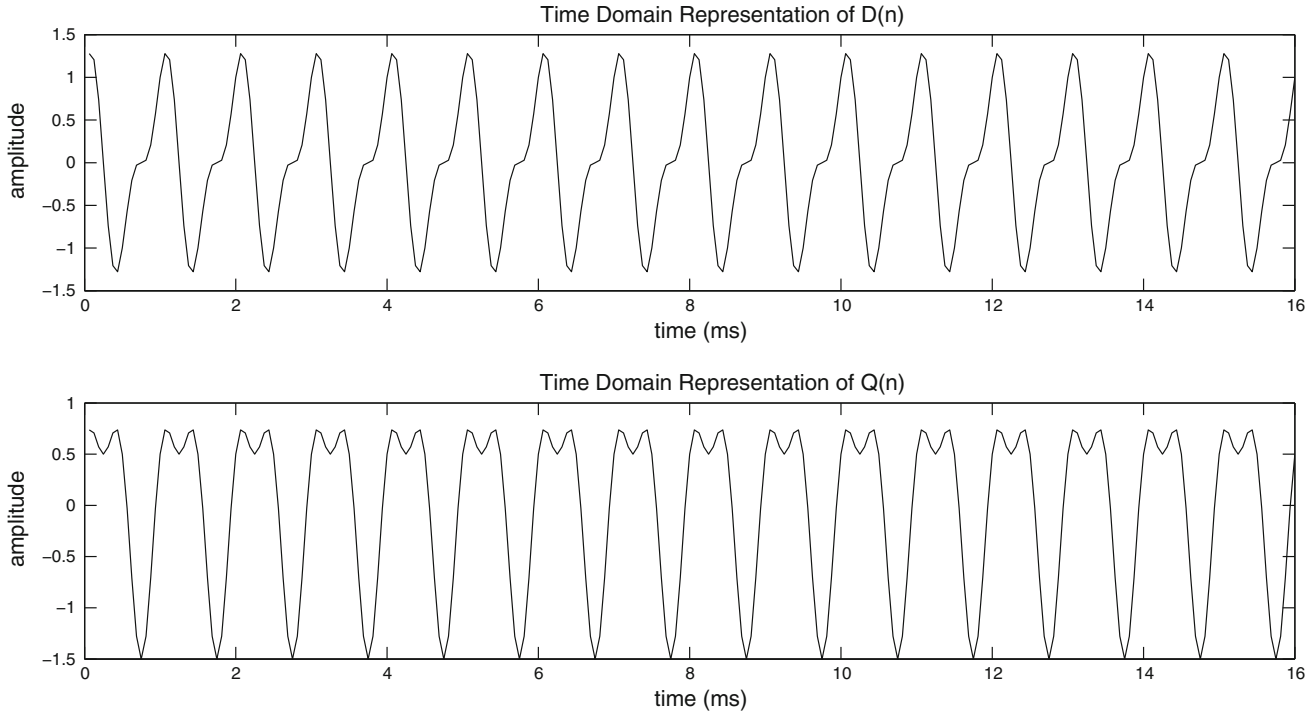

Fig. 5 Time domain representation of the simulated $D(n)$ and $Q(n)$

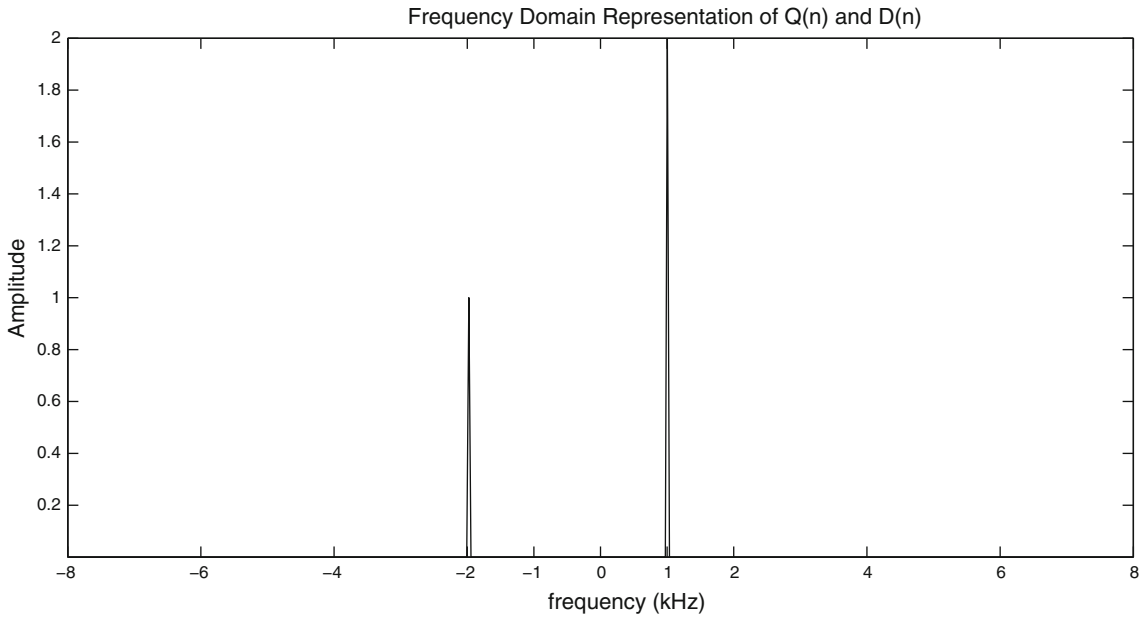

Fig. 6 Frequency domain representation of the simulated $D(n)$ and $Q(n)$

Fig. 6, the impulse seen in positive band represents signal at one direction, and the other impulse seen in negative frequency band represents the other direction [4].

Assuming that the algorithm performances would be affected by the signal frequency being analyzed, the comparison was evaluated repeatedly by using the simulated signal set for 40 different frequency values (from 100 Hz to 4,000 Hz with 100 Hz steps and with a sampling frequency of 40,000 Hz) and for different threshold levels (from 0 to 0.6 with 0.02 steps). The reason for choosing such high sampling frequency is to minimize the effect of sampling frequency on the denoising performances of the methods with changing simulated signal frequencies. Because approximately 7 dB noise level is used as a lower limit value in embolic signal identification [23], the noise levels, which are added to simulation signals, are chosen as 6, 8 and 10 dB for all threshold and frequency values.

For these evaluations, the simulated signal given by Eqs. (8) and (9), where forward and reverse signal amplitudes and frequencies were set to be equal ($A = B, f_A = f_B$), was used. The Matlab function "awgn" is used in order to add white Gaussian noise to our simulation signals. With this function, desired noise levels in dB can be added depending upon the simulation signal power. White Gaussian noise has wide-band spectrum and contains equal-energy components for all frequencies in its spectrum. The idea behind the usage of this type of noise for simulation signals is that if we can prove the denoising performance of MDTCWT for wide-band noise types, it will also mean that it will perform well for band-limited noise types.

As a final step, average RMSE and average SNR values were computed for each threshold level and for each frequency value for three different noise levels. In order to obtain completely unbiased results, the processes described above were done 50 times and mean values of these 50 trials were presented.

4.2 Real signals

In the second part of analysis, 25 embolic signals with particularly low EBR values selected from a data set as described in [5] were used. Recordings of these signals were made from a middle cerebral artery using an axial sample volume of 5 mm. The quadrature ultrasonic Doppler signals had been recorded using a transcranial Doppler system (EME Pioneer TC4040 which is manufactured by Nicolet Biomedical, Madison, USA). The sampling frequency was 7,150 Hz, and the data length was 2,048 point (286 ms). Prior to the recordings, informed consent of each patient was obtained.

For DWT denoising, the filter coefficients used in [18] with five scales were used. For DTCWT denoising and MDTCWT denoising, the DTCWT algorithm given in [29] and the MDTCWT algorithm described in [32] with five scales were used. Because an embolic signal can be considered as narrow-band signal, relatively low number of scales (5 in our case) would be enough.

In [27], it was mentioned that the noise, which appears in Doppler ultrasound systems, has white Gaussian noise characteristics. In decomposition part of wavelet transform, noise shows itself in all subbands and added to emboli information. Therefore, in our method, we calculated a threshold value from the first subband (first detail coefficients), which has the biggest amount of noise, for each

embolic signal by using universal thresholding method and then applied this threshold to all subbands using soft thresholding. The calculated universal thresholding can be formulated as below:

$$T = \sigma_{\text{est}}\sqrt{2\log(N)} \tag{10}$$

where N is the number of samples in embolic signal and σ_{est} represents the standard deviation of noise in the first detail coefficients. σ_{est} can be estimated via median absolute deviation by the following formula:

$$\sigma_{\text{est}} = \frac{\left|\text{median}(c_d^1)\right|}{0.6745} \tag{11}$$

where c_d^1 is the detail coefficients of first level in wavelet decomposition and 0.6,745 is a normalization factor [12].

In order to visualize and measure denoising performance of proposed method, Doppler signals before denoising and after denoising with MDTCWT, DTCWT and DWT were analyzed using 128-point complex FFT with Gaussian window. The TF representation of embolic signals before and after denoising was compared by calculating EBR, HWM as an estimate of temporal resolution and ESO as an estimate of the accuracy of temporal localization [6]. The HWM for the time resolution is defined as the temporal distance between the point at which the IP of embolic signal reached half-maximum and the point at which it fell to half-maximum. In our implementation, the ESO was defined as the time point where IP of the embolic signal reaches 20% of the maximum IP. The HWM and ESO levels for a time domain signal are illustrated as long dashed and short dashed lines, respectively, in Fig. 4.

As mentioned before in Sect. 3, the MDTCWT has the same computational complexity with the DWT and half of the DTCWT for processing quadrature Doppler signals. To prove this property, the denoising computational complexity of the MDTCW was compared with the PFT followed by denoising with two real DWTs, and the PFT followed by denoising with two DTCWTs for one real embolic signal on a PC with Intel(R) Core(TM) Duo CPU 2.26 GHz processor and 4 GB RAM. The algorithms were implemented in Matlab and tested using a quadrature Doppler signal having 2,048 samples. In order to minimize effect of any computational time used by any program, which might be running at the background, each algorithm was run 50,000 times and average execution times of each method were calculated.

5 Results

5.1 Simulation results

Figures 7, 8, 9 and 10 illustrate the average SNR and RMSE values for the MDTCWT, DWT and DTCWT for various threshold levels and frequency levels when 10 dB noise is added. In Figs. 7 and 9, the SNR/RMSE values for

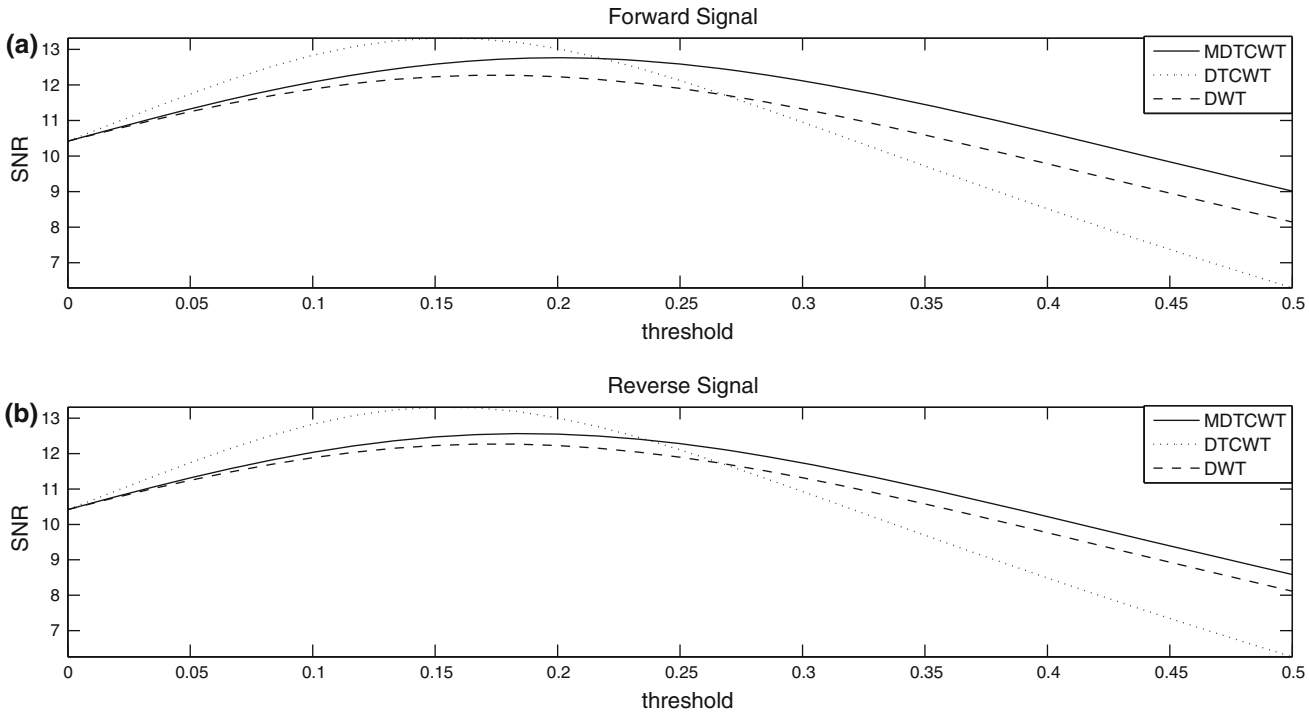

Fig. 7 Average SNR values in dB for MDTCWT, DTCWT and DWT for different threshold levels. **a** Forward signal, **b** reverse signal

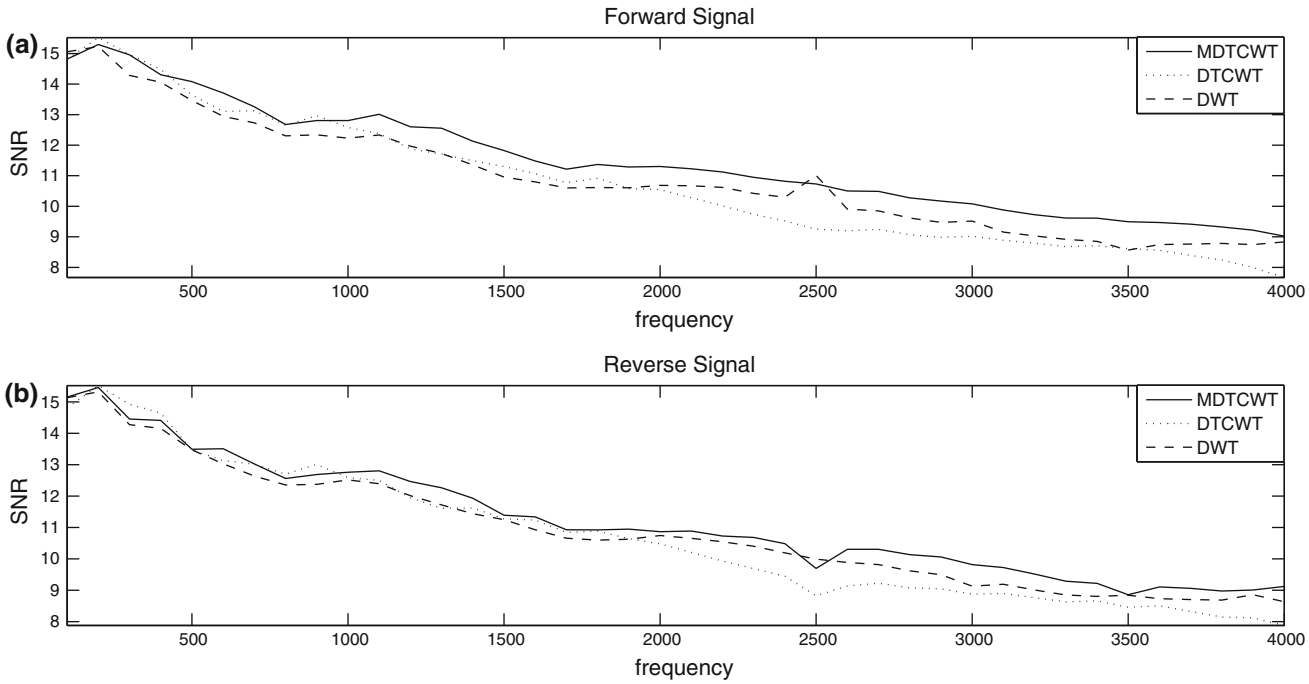

Fig. 8 Average SNR values in dB for MDTCWT, DTCWT and DWT for different frequencies. **a** Forward signal, **b** reverse signal

forward and reverse signals for each threshold level were obtained by taking mean of SNR/RMSE values for 40 different signals with frequencies ranging from 100 to 4,000 Hz with 100 Hz steps and with a sampling frequency of 40,000 Hz. This gives an unbiased denoising performance depending on threshold levels for each algorithm. In Figs. 8 and 10, the SNR/RMSE values for forward and reverse signals for each signal (with different frequencies) were obtained by taking mean of SNR/RMSE values for 30 different threshold levels ranging from 0 to 0.6 with 0.02 steps for each signal. This gives an unbiased denoising performance depending on changing signal frequencies for each algorithm.

Considering the denoising performance of MDTCWT, as can be seen from the figures above, the MDTCWT has better overall denoising performance in both directions than the conventional DWT. When the SNRs of denoised signals for the three methods (Figs. 7, 8) are examined, the MDTCWT gives higher SNRs than the DWT. Although the DTCWT appears to perform best up to a certain level (particularly at low frequencies and low threshold levels), the MDTCWT has the best performance at higher frequencies and threshold levels.

The RMSE metric gives us information about the similarity between the original signals and the denoised signals. When the RMSE values of denoised signals for the three methods (Figs. 9, 10) are examined, the DWT has the worst denoising performance. The DTCWT appears to perform best up to a certain threshold level, and then its performance becomes worst. The MDTCWT consistently gives better RMSE results than the DWT for all threshold levels. It also performs better than the DTCWT after a certain threshold level.

Table 1 shows maximum mean (SD) values of SNR calculations and minimum mean (SD) values of RMSE calculations for three noise levels (6, 8 and 10 dB) in both directions (reverse and forward signals) depending on both frequency and threshold level. As it can be seen from the table, the mean values of SNR and RMSE with the MDTCWT denoising are better than with both the DWT and the DTCWT. Besides, the maximum values of SNR values, which are obtained after the MDTCWT denoising, are higher than the maximum values of the DWT denoising results. In addition, the minimum values of RMSE values, which are obtained after the MDTCWT denoising, are smaller than the minimum values of the DWT denoising results. This shows us that for all three noise levels in both directions of the simulated signals, the MDTCWT gives better denoising performance than the conventional DWT.

5.2 Results with real signals

Without any denoising, mean (SD) values of the EBR, HWM and ESO for the 25 embolic signals were 17.6 (2.31) dB, 9.5 (3.56) ms and 67.8 (7.26) ms, respectively. After denoising using the DWT, mean values of the EBR, HWM and ESO for the 25 embolic signals were 22.19 (3.21) dB, 8.96 (3.62) ms and 70.05 (7.34) ms,

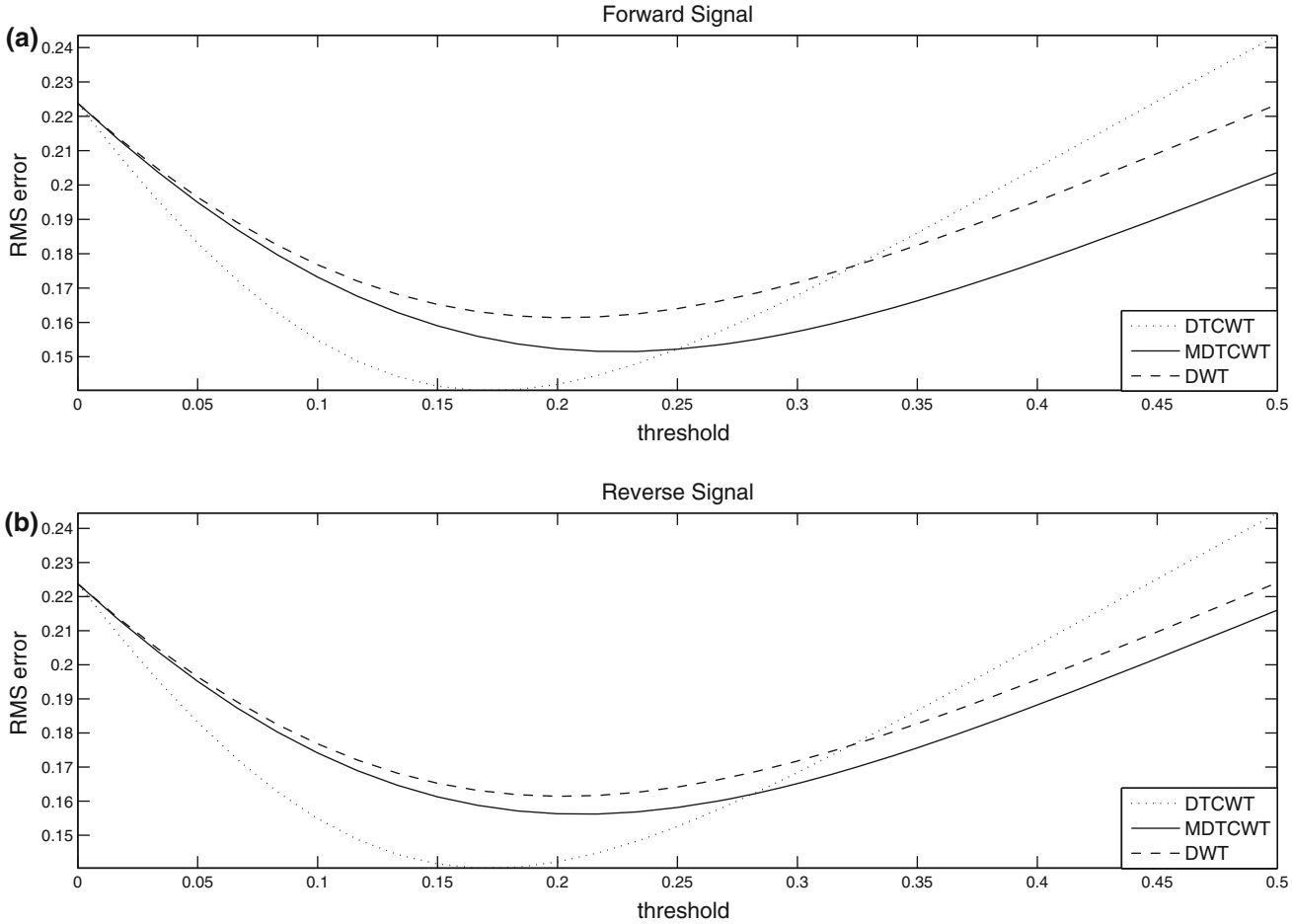

Fig. 9 Average RMSE for MDTCWT, DTCWT and DWT for different threshold levels. **a** Forward signal, **b** reverse signal

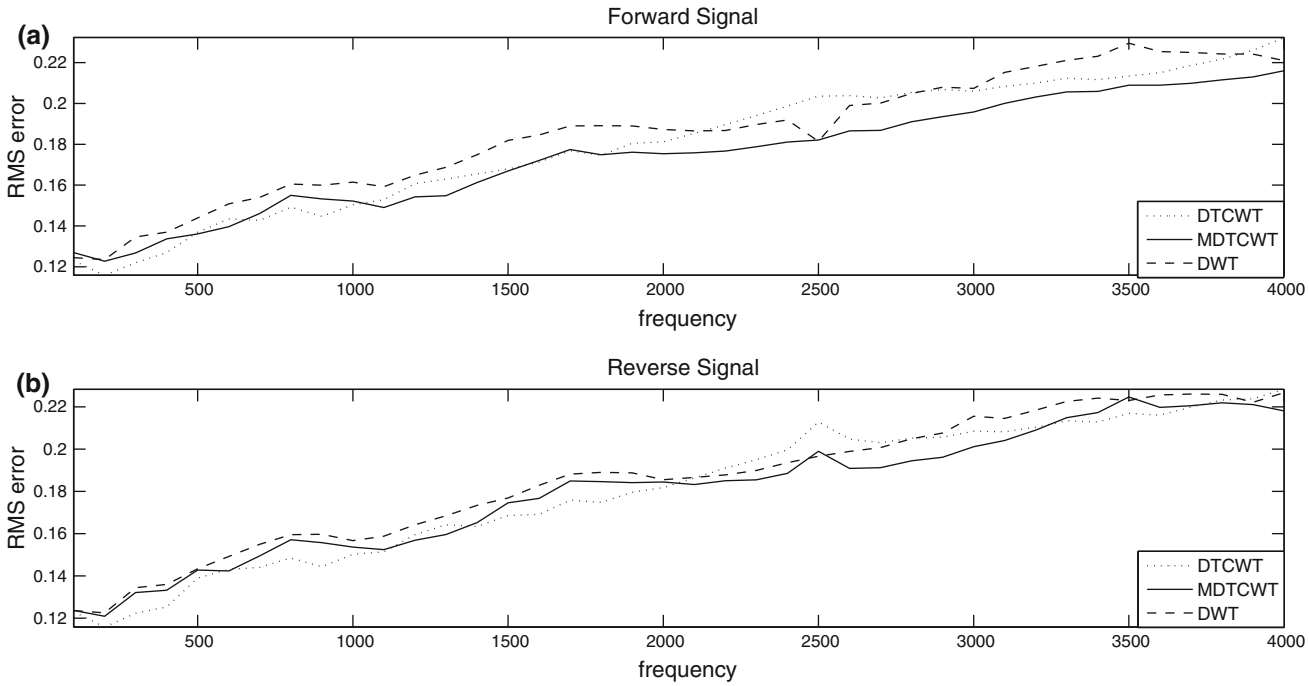

Fig. 10 Average RMSE for MDTCWT, DTCWT and DWT for different frequencies. **a** Forward signal, **b** reverse signal

Table 1 SNR and RMSE values for three noise levels in both directions

	SNR (dB)-threshold		SNR (dB)-frequency		RMS-threshold		RMS-frequency	
	Max	Mean (SD)	Max	Mean (SD)	Min	Mean (SD)	Min	Mean (SD)
6 dB Gaussian noise (forward)								
MDTCWT	8.9910	8.211 (0.6645)	10.9900	8.211 (1.327)	0.2243	0.2565 (0.03786)	0.2059	0.2565 (0.02643)
DTCWT	9.4530	7.745 (1.53)	11.7700	7.745 (1.865)	0.2084	0.2504 (0.03926)	0.1818	0.2504 (0.03483)
DWT	8.6320	7.857 (0.681)	10.9900	7.857 (1.414)	0.2364	0.2655 (0.03333)	0.2043	0.2661 (0.02976)
6 dB Gaussian noise (reverse)								
MDTCWT	8.8550	8.073 (0.6691)	11.2000	8.073 (1.36)	0.2304	0.2609 (0.03548)	0.2028	0.2609 (0.02815)
DTCWT	9.4330	7.725 (1.533)	11.8800	7.725 (1.859)	0.2089	0.2509 (0.0392)	0.1805	0.2509 (0.03486)
DWT	8.6090	7.83 (0.6887)	11.1100	7.83 (1.414)	0.2370	0.2661 (0.03318)	0.2043	0.2661 (0.02976)
8 dB Gaussian noise (forward)								
MDTCWT	10.8700	10.02 (0.7244)	13.1000	10.02 (1.418)	0.1845	0.2088 (0.02715)	0.1611	0.2088 (0.02459)
DTCWT	11.3800	9.611 (1.539)	13.9100	9.611 (1.908)	0.1711	0.2063 (0.03075)	0.1431	0.2063 (0.03149)
DWT	10.4400	9.591 (0.7458)	13.1400	9.591 (1.519)	0.1957	0.2181 (0.02331)	0.1611	0.2181 (0.02791)
8 dB Gaussian noise (reverse)								
MDTCWT	10.6900	9.824 (0.735)	13.1700	9.824 (1.491)	0.1903	0.2138 (0.02506)	0.1597	0.2138 (0.02701)
DTCWT	11.3500	9.574 (1.543)	13.8100	9.574 (1.925)	0.1718	0.2071 (0.03072)	0.1439	0.2071 (0.03183)
DWT	10.4100	9.559 (0.7498)	13.1200	9.559 (1.547)	0.1963	0.2187 (0.02322)	0.1606	0.2187 (0.02839)
10 dB Gaussian noise (forward)								
MDTCWT	12.7600	11.47 (1.122)	15.3000	11.47 (1.756)	0.1516	0.1746 (0.02041)	0.1228	0.1746 (0.02705)
DTCWT	13.3100	10.73 (2.212)	15.5200	10.73 (2.158)	0.1402	0.1804 (0.03261)	0.1159	0.1804 (0.03265)
DWT	12.2700	10.9 (1.256)	15.2300	10.9 (1.846)	0.1614	0.1855 (0.02048)	0.1236	0.1855 (0.03023)
10 dB Gaussian noise (reverse)								
MDTCWT	12.5600	11.21 (1.2)	15.4600	11.21 (1.838)	0.1562	0.1805 (0.02073)	0.1209	0.1805 (0.02977)
DTCWT	13.3100	10.72 (2.224)	15.5200	10.72 (2.177)	0.1404	0.1807 (0.0328)	0.1158	0.1807 (0.03307)
DWT	12.2700	10.89 (1.265)	15.3200	10.89 (1.889)	0.1614	0.1857 (0.02058)	0.1225	0.1857 (0.03094)

"Frequency" means; the calculations are done over frequency dependence and "threshold" means; the calculations are done over threshold dependency

respectively. When the DTCWT was used for the denoising, mean values of the EBR, HWM and ESO for the 25 embolic signals were 25.80 (4.98) dB, 8.85 (3.61) ms and 69.98 (7.33) ms, respectively. When the MDTCWT was used for the denoising, mean values of the EBR, HWM and ESO for the 25 embolic signals were 25.54 (4.75) dB, 8.84 (3.60) ms and 70.20 (7.33) ms, respectively. These results are also tabulated in Table 2.

Comparing the results obtained without denoising, by denoising with the DWT, with the DTCWT and with the MDTCWT, the EBR value of the MDTCWT is as good as the EBR value of the DTCWT, which appears to give the best result. Both methods provide approximately 8 dB improvement, while the conventional DWT provides an improvement less than 5 dB. Figure 11 illustrates the EBR values without denoising and after denoising by each method for 25 embolic signals.

In order to demonstrate the improvement provided by denoising with the DWT, the MDTCWT and the DTCWT in real signals, the denoised signals and original signals were analyzed by using windowed Fourier transform (WFT), resulting in a TF representation of the signals. In the WFT analysis, a Gaussian window with 128-point length was used. The EBR, the ESO and the HWM parameters are calculated by using IP of embolic signals. Therefore, IPs of denoised signals with three methods calculated by integrating TF plane over the frequency [10] were compared with the IP of the original signal.

As an example, Fig. 12 shows counterplots of the TF representation of a noisy embolic signal (b), denoised signal with the MDTCWT (c), the DWT (d) and the DTCWT (e). According to Figs. 7 and 9, denoising performances of the methods are influenced by the choice of the threshold level. Therefore, a TF representation of a denoised signal for a single threshold level may not be a good qualitative indicator of the denoising performance of a method. In order to emphasize this argument, in Fig. 12, the TF representations were constructed by using a signal obtained by averaging denoised signals resulting from denoising the same signal using different threshold levels. These thresholds were determined by multiplying the previously described threshold (Eqs. 10 and 11) with five

Table 2 EBR, HWM and ESO values of three denoising methods

	EBR in dB-mean (SD)	HWM in ms-mean (SD)	ESO in ms-mean (SD)
Without denoising	17.6 (2.31)	9.5 (3.56)	67.8 (7.26)
DWT	22.19 (3.21)	8.96 (3.62)	70.05 (7.34)
DTCWT	25.80 (4.98)	8.85 (3.61)	69.98 (7.33)
MDTCWT	25.54 (4.75)	8.84 (3.60)	70.20 (7.33)

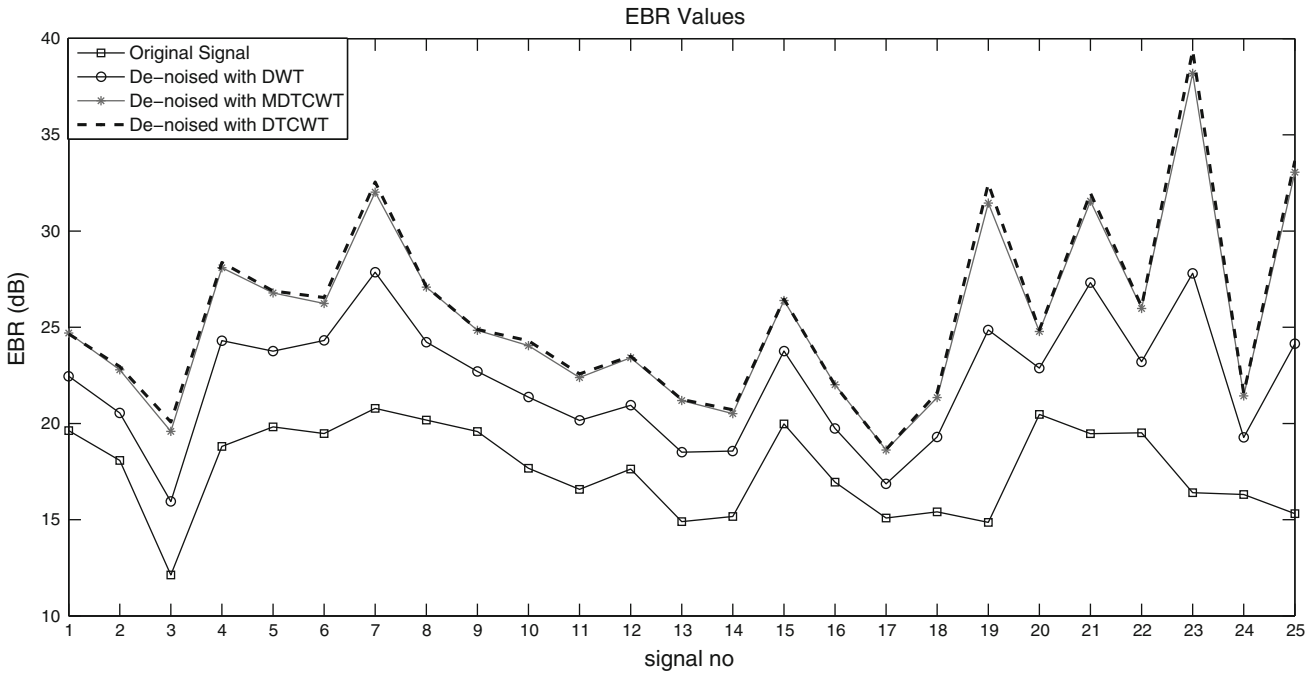

Fig. 11 EBR values for each signal

different constants (0.90, 0.95, 1, 1.05 and 1.10). For clarity, Fig. 13 illustrates the noisy signal and corresponding IP representations of the same signal and the denoised signals with the MDTCWT, the DWT and the DTCWT (in this figure, unlike Fig. 12, a single threshold calculated by using Eqs. 10 and 11 is used). The IP representations were obtained by integrating the TF representations of the denoised signals over the frequency. As it can be seen from Figs. 12 and 13, MDTCWT removes noise and enhances the signal of interest (embolic part) better than the DWT.

The processing times indicating the computational complexities of three denoising methods (the PFT followed by denoising with two DWTs, the PFT followed by denoising with two DTCWTs and denoising with the MDTCWT) can be seen in Table 3. Computational cost of denoising with the MDTCWT (11.6 ms) is almost the same as the PFT followed by denoising with two DWTs (11.1 ms) and half of the PFT followed by denoising with two DTCWTs (20.7 ms).

6 Discussion and conclusion

DWT is a very popular tool for the analysis of biological signals. It is reported in the literature that it was used for processing quadrature Doppler signals previously. However, the DWT lacks shift invariance property, which is important in analysis of the signals in which the phase distortion is not tolerated. In the analysis of embolic quadrature Doppler signals, which are nonstationary and transient, the phase may be distorted by the DWT analysis. The DTCWT was developed to overcome the lack of shift invariance property of conventional DWT. However, prior to applying the DTCWT to the quadrature Doppler signals, first quadrature signals must be decoded into the directional signals and then two DTCWTs should be applied, doubling the computational complexity. The MDTCWT has also near-shift invariance property, but unlike the DTCWT, it is capable of mapping directional signals at the transform output with the reduced computational complexity. Therefore, in this study, in order to benefit from its shift

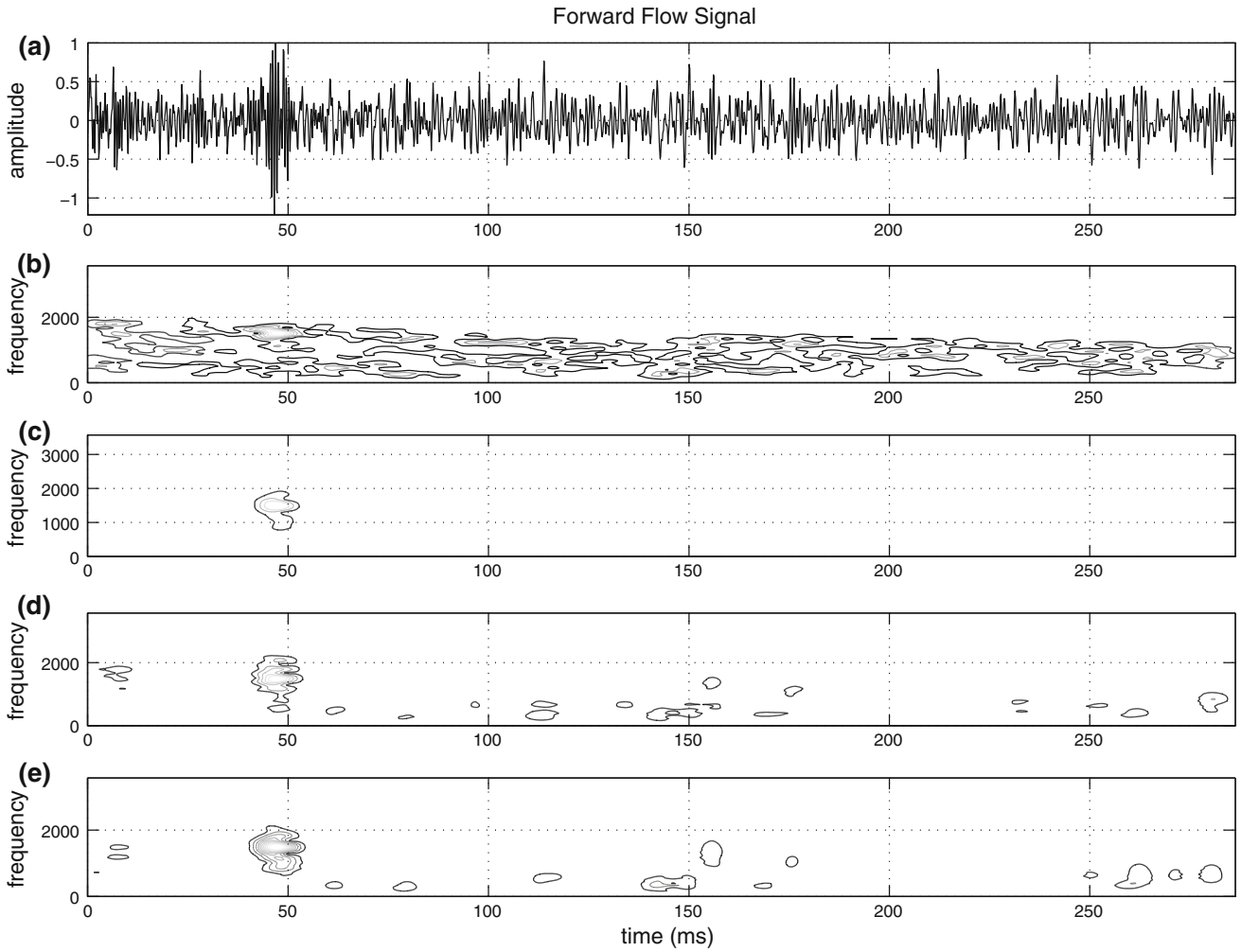

Fig. 12 Counterplot of noisy (**b**) and denoised embolic signals with MDTCWT (**c**), DWT (**d**) and DTCWT (**e**)

Table 3 Processing time comparison of three denoising methods

Denoising method	Processing time (ms)
MDTCWT	11.6
PFT followed by two DWTs	11.1
PFT followed by two DTCWTs	20.7

invariance and computational efficiency properties, simulated and real quadrature signals were denoised with the MDTCWT, and the results were presented.

For both simulated and real signals, denoising with the MDTCWT gave better results than the ordinary DWT and similar results to the DTCWT in both reverse and forward directional signals. In the simulation signals case, the DTCWT had better denoising performance than the MDTCWT for low frequencies and low threshold levels. However, the MDTCWT had the best performance for the high frequencies and high threshold levels. This may be attributed to the fact that in the MDTCWT, denoising operation is performed on quadrature coefficients prior to directional decoding, leading to further possible suppression of noise during synthesis as a result of addition/subtraction operation (averaging). Embolic signals are transient signals, and their frequency spectrum mostly appears in high frequencies. Therefore, denoising with MDTCWT may give better results than the DTCWT in the detection of embolic signals.

In the real embolic signals denoising case, the MDTCWT gave very similar EBR values when compared with the EBR values obtained with the DTCWT and better EBR values than the DWT results for all 25 samples. The EBR is a widely used parameter in detecting embolic signals. So, using the MDTCWT instead of the DWT may increase detection success of analysis with almost the same computational complexity.

As a conclusion, with the MDTCWT there is a notable improvement in denoising quadrature signals performance over the denoising with the DWT with the same

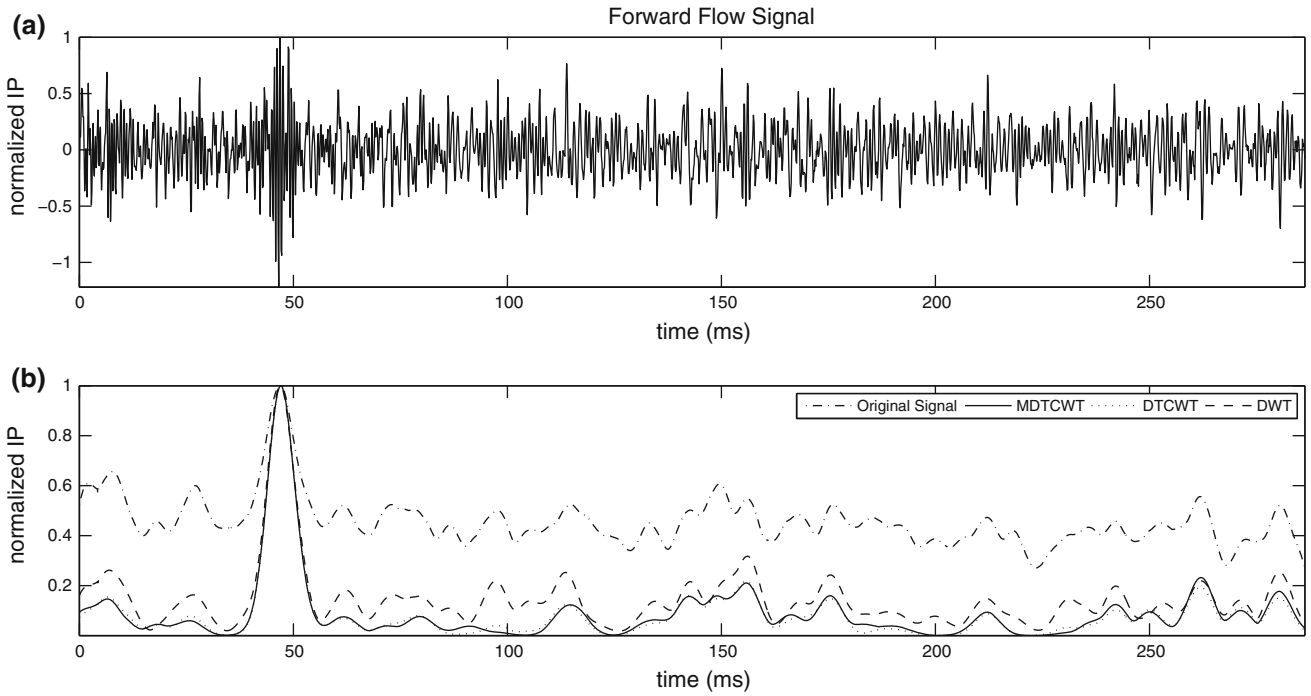

Fig. 13 Noisy embolic signal (**a**) and instantaneous powers of noisy embolic signal and denoised signals with MDTWT, DWT and DTCWT (**b**)

computational complexity. It is clear that the MDTCWT appears to increase embolic signal conspicuity as good as the DTCWT and better than the conventional DWT. This method can be used in different signal processing applications where the quadrature demodulation is used and quadrature signals are obtained. In the future, this algorithm can also be integrated to online embolic signal detection and classification algorithms and is expected to improve detection and classification of signals particularly caused by very small asymptomatic emboli.

References

1. Achim A, Bezerianos A, Tsakalides P (2001) Novel Bayesian multiscale method for speckle removal in medical ultrasound images. IEEE Trans Med Imaging 20(8):772–783
2. Ackerstaff RG, Babikian VL, Georgiadis D, Russell D, Siebler M, Spencer MP, Stump D (1995) Basic identification criteria of Doppler microembolic signals. Stroke 26:1123
3. Aydin N, Evans DH (1994) Implementation of directional Doppler techniques using a digital signal processor. Med Biol Eng Comput 32:157–164
4. Aydin N, Fan L, Evans DH (1994) Quadrature-to-directional format conversion of Doppler signals using digital methods. Physiol Meas 15:181–199
5. Aydin N, Marvasti F, Markus HS (2002) Effect of wavelet denoising on time-frequency and time-scale analysis of quadrature embolic signals. In: Proceedings of 24th annual international conference of the IEEE engineering in medicine and biology society, Houston, pp 80–81
6. Aydin N, Marvasti F, Markus HS (2004) Embolic Doppler ultrasound signal detection using discrete wavelet transform. IEEE Trans Inf Tech Biomed 8(2):182–190
7. Boashash B (1992) Estimating and interpreting the instantaneous frequency of a signal: a tutorial review—part 2: algorithms and applications. Proc IEEE 80:539–568
8. Brigham EO (1974) The fast Fourier transform. Prentice Hall Inc, Englewood Cliffs, NJ
9. Chang SG, Yu B, Vetterli M (2000) Adaptive wavelet thresholding for image denoising and compression. Trans Image Process 9(9):1532–1546
10. Cohen L (1989) Time-frequency distributions—a review. Proc IEEE 77(7):941–981
11. Donoho DL (1995) Denoising by soft-thresholding. IEEE Trans Inf Theory 41:613–647
12. Donoho DL, Johnstone IM (1994) Ideal spatial adaptation via wavelet shrinkage. Biometrika 81:425–455
13. Donoho DL, Johnstone IM (1995) Adapting to unknown smoothness via wavelet shrinkage. J Am Stat Assoc 90(432):1200–1224
14. Donoho DL, Johnstone IM (1998) Minimax estimation via wavelet shrinkage. Ann Stat 26(3):879–921
15. Evans DH, McDicken WN, Skidmore R, Woodcock JP (1989) Doppler Ultrasound: Physics, Instrumentation and Clinical Applications. Wiley, Chichester
16. Fan L, Evans DH, Naylor AR, Tortoli P (2004) Real-time identification and archival of microembolic Doppler signals using a knowledge-based system. Med Biol Eng Comput 42:193–204
17. Kingsbury NG (1998) The dual-tree complex wavelet transform: a new technique for shift invariance and directional filters. IEEE Digital Signal Process Workshop Bryce Canyon 86:319–322

18. Kingsbury NG (1999) Image processing with complex wavelets. Philos Trans R Soc Lond A 357:2543–2560
19. Krim H, Tucker D, Mallat S, Donoho D (1999) On denoising and best signal representation. IEEE Trans Inf Theory 45(7):2225–2238
20. Li H, Zhang Y, Xu D (2010) Noise and speckle reduction in Doppler blood flow spectrograms using an adaptive pulse-coupled neural network. EURASIP J Adv Signal Process. doi:10.1155/2010/918015
21. Markus H (1993) Transcranial Doppler detection of circulating cerebral emboli. A review. Stroke 24(8):1246–1250
22. Markus HS, Harrison MJ (1995) Microembolic signal detection using ultrasound. Stroke 26:1517–1519
23. Markus HS, Molloy J (1997) The use of a decibel threshold in the detection of embolic signals. Stroke 28:692–695
24. Markus HS, Reid G (1999) Frequency filtering improves ultrasonic embolic signal detection. Ultrasound Med Biol 25:857–860
25. Markus H, Loh A, Brown MM (1993) Computerized detection of cerebral emboli and discrimination from artifact using Doppler ultrasound. Stroke 24(11):1667–1672
26. Marvasti S, Gillies D, Marvasti F, Markus HS (2004) Online automated detection of cerebral embolic signals using a wavelet based system. Ultrasound in Med Biol 30:647–653
27. Marvasti S, Gillies D, Markus HS (2004) Novel intelligent wavelet filtering of embolic signals from TCD ultrasound. Conference record of the thirty-eighth Asilomar conference on signals, systems and computers, vol 2, pp 1580–1584
28. Pasti L, Walczak B, Massart DL, Reschiglian P (1999) Optimization of signal denoising in discrete wavelet transform. Chemom Intell Lab Syst 48:21–34
29. Selesnick IW, Baraniuk RG, Kingsbury NG (2005) The dual-tree complex wavelet transform. IEEE Signal Process Mag 22(6):123–151
30. Serbes G, Aydin N, (2009) A complex discrete wavelet transform for processing quadrature Doppler ultrasound signals. In: 9th international conference on information technology and applications in biomedicine ITAB 2009
31. Serbes G, Aydin N, (2010) Denoising performance of modified dual tree complex wavelet transform. In: 10th international conference on information technology and applications in biomedicine ITAB 2010, pp 1–4
32. Serbes G, Aydin N (2011) Modified dual tree complex wavelet transform for processing quadrature signals. Biomed Signal Process Control 6(3):301–306
33. Spencer MP, Thomas GI, Nicholls SC, Sauvage LR (1990) Detection of middle cerebral artery emboli during carotid endarterectomy using transcranial Doppler ultrasonography. Stroke 21:415–423
34. Taswell C (2000) The what, how, and why of wavelet shrinkage denoising. Comput Sci Eng 2(3):12–19
35. Yoon BJ, Vaidyanathan PP (2004) Wavelet-based denoising by customized thresholding. IEEE Int Conf Acoust Speech Signal Process 2:925–928
36. Zhang Y, Wang L, Gao Y, Chen J, Shi X (2007) Noise reduction in Doppler ultrasound signals using an adaptive decomposition algorithm. Med Eng Phys 29(6):699–707